RSC Advances

ROYAL SOCIETY OF CHEMISTRY

www.rsc.org/advances

Journal Name

COMMUNICATION

Controllable Synthesis of Porous Iron-Nitrogen-Carbon Nanofibers with Enhanced Oxygen Reduction Electrocatalysis in Acidic Medium

Received 00th January 20xx,
Accepted 00th January 20xx

DOI: 10.1039/x0xx00000x

www.rsc.org/

X. X. Yan,[a] L. Gan,[a] F. Fang,[a] K. X. Liu,[a] J. Luo,*[a] and J. Zhu*[a]

We synthesized porous Fe-N-C nanofibers as non-precious metal catalysts to investigate the impact of surface area on electrocatalysis performance. The surface area was modified by adjusting the proportion of the added silicon nanoparticles, and achieved a 20-times enhancement of the electrocatalysis performance at an optimized proportion.

As one of the most significant problem nowadays, energy crisis has aroused wide researches on new energy conversion devices, such as fuel cells (FCs).[1-3] However, the commercialization and widespread application of FCs are seriously restricted by plenty usage of the expensive platinum-based catalysts, which have been applied to improve the sluggish kinetics of oxygen reduction reaction (ORR) in the cathode.[4,5] Various types of non-precious metal (NPM) catalysts with low cost have been discovered and developed to replace those Pt-based catalysts for many decades.[6-9] Among them, the most promising alterative of Pt-based catalysts are those which contain active sites of transition metal coordinated with nitrogen atoms (TM-N_x) on carbon supports, especially when the medium is acidic, in order to match the condition of proton exchange membrane fuel cell (PEMFC).[10-14] Since the first report of such ORR-activated structure in 1964,[6] such NPM catalysts have achieved great improvement during the last decade.[10-12] These researches pointed out that the surface area and active sits played signification roles in electrocatalysis performance. However, in the reported impregnation method,[10-12] there is still a tradeoff remained between the surface area and the active sites. For one thing, the process of absorbing active sites will cause an obvious drop of surface area.[11,15] For another, the treatment of increasing surface area will damage the active sites.[16] Ammonia treatment has be developed to supply nitrogen atoms for remaining active sites in company with increasing surface area.[11,17] But ammonia is dangerous and environmental friendless. Hence, it seems that is difficult to obtain both the high surface area and the abundant active sites at the same time. In this work, we have brought up a new type of porous iron-nitrogen-carbon (Fe-N-C) nanofibers as NPM catalyst by removing silicon nanoparticles (Si NPs) in carbon nanofibers, which were employed to create porous structure and then acquire high surface area and plenty of active sites. We applied them in the acidic medium, and revealed that the electrocatalysis performance of these catalysts could be enhanced after etching Si NPs and controlled by modifying additional porous structure. Combining with transmission electron microscopy (TEM) observation, we further found that, with the increment of the weight proportion of Si NPs, the electrochemical performances of various porous catalysts were first enhanced and then dropped down, for the aggregation of Si NPs.

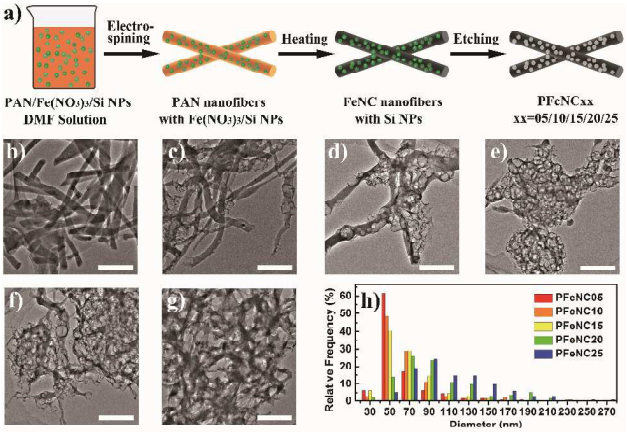

Fig. 1 (a) Schematic diagram of the synthesis of porous Fe-N-C nanofibers by electrospinning, heating and etching Si NPs (green balls). (b-g) The typical TEM images of FeNC, PFeNC05, PFeNC10, PFeNC15, PFeNC20, and PFeNC25 samples, respectively. The scale bars are all 500 nm. (g) Histograms between the relative frequency and pore diameters of PFeNC05, PFeNC10, PFeNC15, PFeNC20, and PFeNC25, respectively.

As depicted in Fig. 1a, porous Fe-N-C nanofibers were synthesized by first electrospinning the polyacrylonitrile (PAN) nanofibers

[a] National Center for Electron Microscopy in Beijing, Key Laboratory of Advanced Materials (MOE) and The State Key Laboratory of New Ceramics and Fine Processing, School of Materials Science and Engineering, Tsinghua University, Beijing 100084, China
E-mail: luojunkink@126.com; jzhu@mail.tsinghua.edu.cn
Electronic Supplementary Information (ESI) available: Experimental Details and Fig. S1-S2. See DOI: 10.1039/x0xx00000x

containing ferric nitrate and Si NPs,[18,19] then heating the as-electrospun nanofibers to get carbon nanofibers,[20,21] and finally etching Si NPs in alkaline solution (typically 3M KOH) to create the expected porous structure (see experimental details in ESI). Our method is compatible with carbon fiber industry, as the major precursor is PAN, which is an easy acquired industrial materials.[22] The weight ratio of Si NPs and PAN (*x*=Si/PAN) was set from 0 to 2.5, with a step of 0.5, and therefore final samples were named as PFeNC05, PFeNC10, PFeNC15, PFeNC20 and PFeNC25, respectively. Sample named FeNC was the one without adding Si NPs and etching process.

Fig. 1b depicts TEM image of FeNC sample without porous structure. FeNC samples were mainly nanofibers, with about 200 nm in diameter. Fig. 1c-g denote the TEM images of samples with various Si/PAN, as PFeNC05, PFeNC10, PFeNC15, PFeNC20, and PFeNC25, indicating that the samples also kept the nanofiber morphology and appeared pores in the nanofibers. Because of relative low proportion of added Si NPs, the pores of PFeNC05 were distributed sparsely as shown in Fig. 1c, matching with the TEM image before etching in Fig. S1a of ESI. With the increment of Si/PAN, the density of distributed pores was increased. The samples with high Si/PAN contained even denser pores in the nanofibers, as depicted in Fig. 1e-g. After detail calibration of pore diameters, we compared different histograms between the relative frequency and the pore diameter of PFeNC05, PFeNC10, PFeNC15, PFeNC20, and PFeNC25 in Fig. 1h. The maximum distribution of pore diameters of PFeNC05 was about 50 nm. Thus, the Si NPs were dispersed separately in the nanofibers of PFeNC05. But, some values of pore diameters of PFeNC05 were higher than 50 nm, indicating that some part of the Si NPs aggregated in nanofibers. The mean pore diameters ($<D_p>$) of PFeNC05, PFeNC10, PFeNC15, PFeNC20, and PFeNC25 were 62, 66, 68, 97 and 112 nm, respectively. These data manifest that the aggregation probability of the Si NPs in the nanofibers became higher, after adding more Si NPs. This could be related to space limitation in the cross-section of nanofiber structure. Fig. S1b in ESI shows TEM image of PFeNC15 samples before etching, indicating that the aggregation of Si NPs could cause the distortion of nanofibers. Figs. S2-4 in ESI provide more TEM images of PFeNC15, PFeNC20 and PFeNC25 to complement those in Fig. 1e-g, manifesting that the morphology of nanofibers was kept with many large pores. The maximum value of the pore diameter reached 270 nm, which was equal to the size of at least 38 Si NPs aggregation (Fig. S5 in ESI). This large aggregation may be explained by the small particles coagulation in the fluid precursor solution during electrospinning process.[23,24,25]

After heating treatment, PAN can convert to conjugated C=C conjugation structure with doped nitrogen, which can be coordinated with iron to form Fe-N_x active site, with results of thermal gravimetric analysis (TGA), fourier transform infrared spectroscopy (FTIR) and X-ray photoelectron spectroscopy (XPS) in Fig. S6 of ESI.[26-29] Fig. 2 indicates the electrochemical measurement of porous Fe-N-C nanofiber catalysts in acidic medium (0.1 M $HClO_4$ solution). In such medium, ORR happened following the reaction equation of $O_2+4H^++4e^-=2H_2O$.[4] Fig. 2a denotes that, after etching Si NPs, the current density of PFeNC05 was increased from 0.037 mA/cm^2 (0 h) to 0.237 mA/cm^2 (72 h) at 0.6 V versus reversible hydrogen electrode (RHE), and enhanced by 6.4 times. With longer etching time, the current density was higher, indicating that more porous structure could increase the electrocatalysis performance. In our experimental condition, the best etching time was about 72 h to remove Si NPs entirely, and further etching couldn't increase the performance. TEM observation of etched samples in Fig. 1c-g also confirmed that no Si NPs were remained in nanofibers. In order to exclude the etching effect on carbon nanofiber matrix, we utilized the same method to treat FeNC sample. Polarization curves of the FeNC without and with etching treatment were almost the same, as displayed in Fig. 2b. Therefore, the enhancement of current density in Fig. 2a was majorly caused by additional surface area of porous structure. Furthermore, scanning electron microscopy (SEM) images and energy dispersive X-ray (EDX) spectra of PFeNC05 samples before and after creating pores are shown in Fig. 2c-f. From SEM images in Fig. 2c and 2e, the samples were kept the nanofiber morphology as same as the TEM observation, and Si NPs were totally removed after etching 72 h from EDX results in Fig. 2d and 2f. Furthermore, element contents from XPS analysis in Table S1 of ESI denote that, after etching, Si atoms were almost removed, matching with the EDX results, and iron atoms were decreased. The etching process could remove the inactive compound containing iron, which have no ORR activity. [12] This explanation could be confirmed by the results in Fig. 2b, which manifested that etching treatment could not affect the ORR activity of the FeNC samples before and after etching treatment.

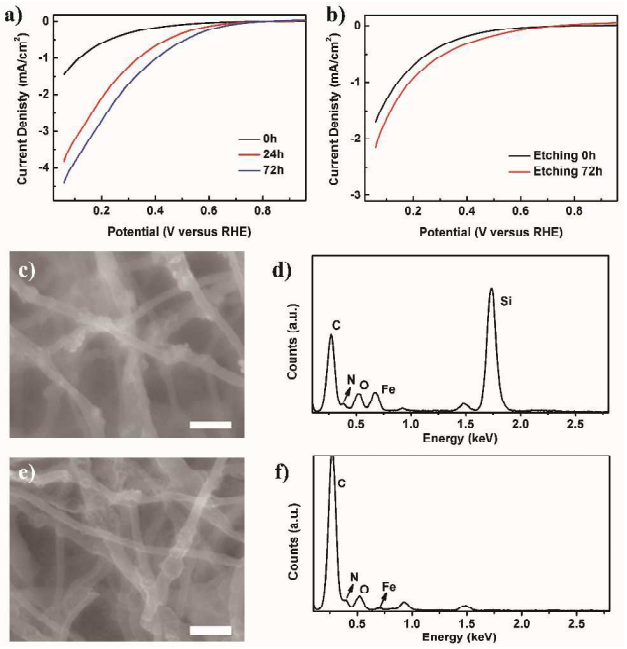

Fig. 2 Results of etching Si NPs in the nanofibers. (a) The linear sweep voltammetry (LSV) curves of PFeNC05 samples with different etching time. (b) The LSV curves of FeNC samples without and with etching process. (c, d) SEM image of nanofibers without etching, and the corresponding EDX spectrum. (e, f) SEM image of nanofibers after etching 72 h, and the corresponding EDX spectrum. The scale bars in (c) and (e) are 500 nm.

Fig. 3a shows the electrochemical performances of all porous catalysts FeNC, PFeNC05, PFeNC10, PFeNC15, PFeNC20, and PFeNC25. Comparing with other porous Fe-N-C nanofiber catalysts, FeNC sample had the lowest performance. For further comparison of various polarization curves, we plot the absolute current density at 0.6 V versus RHE against Si/PAN in Fig. 3b. With the increment of Si/PAN, the absolute current densities of ORR were first enhanced, reached the maximum value of 0.80 mA/cm^2 at Si/PAN=1.5, and then dropped down. Comparatively, the maximum current density of the porous catalysts was 20 times that of FeNC catalysts (0.39 mA/cm^2). As reported, the performance is relevant to the surface area.[11,13,27] The current density was suspected to keep increasing after adding more Si NPs. However, the experimental results indicates that there was an optimized value of Si/PAN. Combination with TEM observation, aggregation may limit the enhancement of porous structure. It can be concluded that total specific surface area (SSA) of porous catalysts (S) is consisted with the SSA of nanofibers (S_{NF}) and the additional SSA of porous structure (S_P):

$$S = S_{NF} + S_P . \quad (1)$$

S_{NF} was proved to be same in various samples, as the etching process didn't affect the surface area of the carbon nanofibers as discussed above, and could be calculated in cylinder model:

$$S_{NF} = \frac{4}{\rho_{NF} D_{NF}}, \quad (2)$$

where ρ_{NF} is the density of nanofibers (ρ_{NF} = 1.7 g/cm^3)[19,20] and D_{NF} is the diameter of nanofibers (D_{NF} = 200 nm). And S_P can be computed by that of the initial Si NPs as:

$$S_P = \frac{x}{\varepsilon} \cdot \frac{6\varphi}{\rho_{Si} \langle D_P \rangle}, \quad (3)$$

where x is the weight ratio of Si and PAN (Si/PAN), ε is the weight shrinkage of PAN nanofibers after heating process (typically ε = 0.4)[20,21,30], φ is the fill factor of Si NPs under close package model (φ = 0.74, Fig S1), ρ_{Si} is the density of silicon (ρ_{Si} = 2.33 g/cm^3),[31] and $\langle D_P \rangle$ is the mean value of pore diameters in nm. Hence, the total SSA of porous Fe-N-C nanofibers can be derived as:

$$S = 11.76 + \frac{4764x}{\langle D_P \rangle}, \quad (4)$$

which was displayed in Fig. 3b. The measured SSA values were in the same range of the calculated ones (Fig. S7 in ESI). Interestingly, the changing mode of calculated SSA was almost same as that of absolute current density of various samples. When Si/PAN was increased from 0 to 1.5, the calculated SSA values increased, and then fell down. The maximum value of calculated SSA of porous catalysts reached 116.7 m^2/g, which was 10 times that of FeNC catalysts. The above results indicate that the initial increment of SSA is caused by adequate porous structure from removing more Si NPs, but the drop of SSA is caused by the aggregation of Si NPs, which lowers the surface area contribution of each added Si NPs.

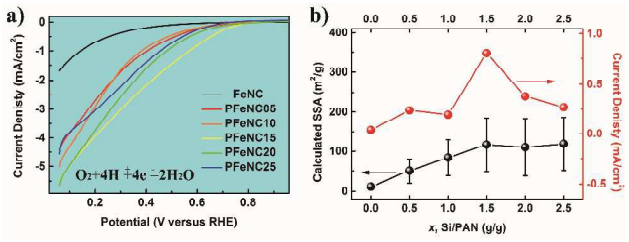

Fig. 3 (a) The LSV curves of FeNC, PFeNC05, PFeNC10, PFeNC15, PFeNC20, and PFeNC25, respectively. (b) The dependences of current density at 0.6 V versus RHE and the calculated SSA from the mean pore diameter in the nanofibers on weight ratio of Si NPs and PAN (Si/PAN).

Furthermore, we normalized the activities (current densities) of all samples by calculated SSA. Fig. S8 in ESI shows that all normalized values were same as each other, indicating that the ORR performance difference was only caused by SSA. It could be inferred that only surface areas of various samples were different, and active sites of Fe-N_x were almost not changed after etching treatment, in our experiments. Hence, the new surface created by removing Si NPs were also distributed with the active sites. And the catalysis activity of porous catalysts had a positive relationship with the surface area of the additional pores, whose pore sizes were 50 nm and larger. For this deduction, some researchers hold the view that the catalysis activity was proportion against the microporous surface area of the catalysts, whose pore size was less than 2 nm.[13,27] Then, we suggested that not only the micropores but also the larger pores can provide the surface area with the active sites and improve the mass transport of substance and production. More importantly, there is an optimization of such additional surface area from etching NPs. In our experiments, the optimized weight ratio of Si NPs and PAN was 1.5, which enhanced calculated specific surface area and current density 10-fold and 20-fold, respectively.

Conclusions

In summary, we synthesized porous Fe-N-C nanofibers as non-precious metal catalysts by a facile and low-cost method. The porous structure can be created by etching the added silicon nanoparticles in the nanofibers, without affecting carbon nanofibers. The current density of etching nanofibers was increasing with longer etching time. Furthermore, the surface area was controlled by modifying the proportion of the added Si nanoparticles, and realized 20 times enhancement of the electrocatalysis performance at an optimized weight ratio of Si NPs and PAN (Si/PAN = 1.5). These results indicated that the porous structure with sizes of about 50 nm could improve the surface area of the nanofibers and enhance the electrocatalysis performance. Nevertheless, this method can also be applied to increase both surface area and active site for more fields.

Notes and references

‡ Acknowledgements. This work was financially supported by National 973 Project of China (2015CB654902), Chinese National

Natural Science Foundation (11374174, 51390471 and 51102145), and National Program for Thousand Young Talents of China. This work made use of the resources of National Center for Electron Microscopy in Beijing.

1 B. C. H. Steele and A. Heinzel, *Nature*, 2001, **414**, 345-352.
2 N. Demirdöven and J. Deutch, *Science*, 2004, **305**, 974-976.
3 U. Eberle, B. Müller and R. von Helmolt, *Energ. Environ. Sci.*, 2012, **5**, 8780-8798.
4 L. Carrette, K. A. Friedrich and U. Stimming, *ChemPhysChem*, 2000, **1**, 162-193.
5 J. K. Nørskov, J. Rossmeisl, A. Logadottir, L. Lindqvist, J. R. Kitchin, T. Bligaard and H. Jónsson, *J. Phys. Chem. B*, 2004, **108**, 17886-17892.
6 R. Jasinski, *Nature*, 1964, **201**, 1212-1213.
7 N. A. Vante and H. Tributsch, *Nature*, 1986, **323**, 431-432.
8 Y. Y. Liang, Y. G. Li, H. L. Wang, J. G. Zhou, J. Wang, T. Regier and H. J. Dai, *Nat. Mater.*, 2011, **10**, 780-786.
9 M. Risch, K. A. Stoerzinger, S. Maruyama, W. T. Hong, I. Takeuchi and Y. Shao-Horn, *J. Am. Chem. Soc.*, 2014, **136**, 5229-5232.
10 R. Bashyam and P. Zelenay, *Nature*, 2006, **443**, 63-66.
11 M. Lefèvre, E. Proietti, F. Jaouen and J. P. Dodelet, *Science*, 2009, **324**, 71-74.
12 G. Wu, K. L. More, C. M. Johnston and P. Zelenay, *Science*, 2011, **332**, 443-447.
13 F. Jaouen, M. Lefèvre, J. P. Dodelet and M. Cai, *J. Phys. Chem. B*, 2006, **110**, 5553-5558.
14 Z. Liu, G. Zhang, Z. Lu, X. Jin, Z. Chang and X. Sun, *Nano Res.*, 2013, **6**, 293-301.
15 G. S. Chai, I. S. Shin and J. S. Yu, *Adv. Mater.*, 2004, **16**, 2057-2061.
16 G. Faubert, R. Côté, J. P. Dodelet, M. Lefèvre and P. Bertrand, *Electrochim. Acta*, 1999, **44**, 2589-2603.
17 J. Yin, Y. J. Qiu and J. Yu, *Electrochem. Commun.*, 2013, **30**, 1-4.
18 M. Inagaki, Y. Yang and F. Y. Kang, *Adv. Mater.*, 2012, **24**, 2547-2566.
19 X. X. Yan, L. Gan, Y.-C. Lin, L. Bai, T. Wang, X. Q. Wang, J. Luo and J. Zhu, *Small*, 2014, **10**, 4072-4079.
20 W. X. Zhang, J. Liu and G. Wu, *Carbon*, 2003, **41**, 2805-2812.
21 J. B. Donnet and R. C. Bansal, *Carbon Fibers*, Marcel Dekker, New York, 1984.
22 E. Frank, L. M. Steudle, D. Ingildeev, J. M. Spörl and M. R. Buchmeiser, *Angew. Chem. Int. Edit.*, 2014, **53**, 5262-5298.
23 D. A. Weitz and M. Oliveria, *Phys. Rev. Lett.*, 1984, **52**, 1433-1436.
24 Y. M. Xuan, Q. Li and W. F. Hu, *AIChE J.*, 2003, 49, 1038-1043.
25 A. Serov, K. Artyushkova and P. Atanassov, *Adv. Energy Mater.*, 2014, 4, 1301735.
26 S. Dalton, F. Heatley and P. M. Budd, *Polymer*, 1999, **40**, 5531-5543.
27 F. Jaouen, J. Herranz, M. Lefèvre, J. P. Dodelet, U. I. Kramm, I. Herrmann, P. Bogdanoff, J. Maruyama, T. Nagaoka, A. Garsuch, J. R. Dahn, T. Olson, S. Pylypenko, P. Atanassov and E. A. Ustinov, *ACS Appl. Mater. Inter.*, 2009, **1**, 1623-1639.
28 L. F. Lai, J. R. Potts, D. Zhan, L. Wang, C. K. Poh, C. H. Tang, H. Gong, Z. X. Shen, L. Y. Lin and R. S. Ruoff, *Energ. Environ. Sci.*, 2012, **5**, 7936-7942.
29 S. Gupta, D. Tryk, I. Bae, W. Aldred and E. Yeager, *J. Appl. Electrochem.*, 1989, **19**, 19-27.
30 X. X. Yan, K. X. Liu, X. Q. Wang, T. Wang, J. Luo and J. Zhu, *Nanotechnology*, 2015, **26**, 165401.
31 D. R. Lide, *CRC Handbook of Chemistry and Physics*, CRC Press, Boca Raton, FL, 82nd edn., 2002.

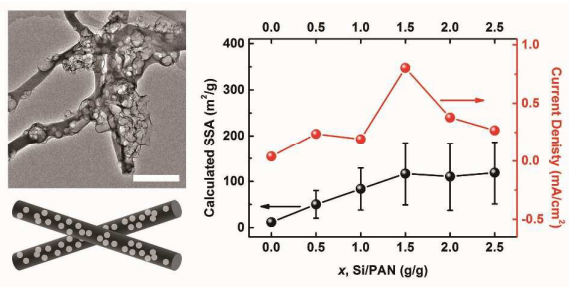

Porous Fe-N-C nanofibers were synthesized as non-precious metal electrocatalysts with a 20-times enhancement of oxygen reduction performance.